XVI International Conference on Computational Plasticity. Fundamentals and Applications
COMPLAS 2021
E. Oñate, D. Peric, M. Chiumenti and Eduardo de Souza Neto (Eds)

MOR OF PIEZOELECTRIC BEAM FEM MODEL AND ITS CONTROL

VLADIMÍR KUTIŠ*, JURAJ PAULECH*, GABRIEL GÁLIK*, JUSTÍN MURÍN* AND VLADIMÍR GOGA*

*Institute of Automotive Mechatronics,
Faculty of Electrical Engineering and Information Technology,
Slovak University of Technology in Bratislava,
Ilkovičova 3, 812 19 Bratislava 1,
Slovak Republic.
e-mail: vladimir.kutis@stuba.sk, web page: http://uamt.fei.stuba.sk/web/

Key words: Finite Element Method, Model Order Reduction, Linear Quadratic Regulator, Piezoelectric Beam Element, Modal Truncation Method

Abstract. The paper deals with the development of the FEM model of piezoelectric beam elements, where the piezoelectric layers are located on the outer surface of the beam core, which is made of functionally graded material. The created FEM model is reduced using the modal truncation method and the results obtain from reduced state-space model are compared with results obtain from finite element model. MOR state-space model is also used in the design of the LQR controller.

1 INTRODUCTION

Smart materials are a very important building blocks in mechatronic applications [1]. These materials include shape memory materials, magnetorheological, functionally graded, piezoelectric, and other types of modern materials [2]. Their main feature is their possibility to extend the functional usage of a given system, to modify the dynamic behavior of a given system or to allow a return to the original state of the system under certain conditions.

Frequently used smart materials are piezoelectric materials, which couple the mechanical and electrostatic fields. This physical coupling predetermines piezoelectric materials for use as sensors or actuators [3], they allow the mechanical deformation to be converted to an electric potential and electrical potential for mechanical deformation, respectively. Such use of piezoelectric materials in mechatronic systems is closely connected to control systems and controller design according to defined requirements. In mechatronic systems the so-called modern control is frequently used [4]. State-space model of a given physical system is used in the design of controllers using modern control theory. From a control viewpoint, it is very desirable that the state-space model is not too large. The finite element method [5] is most often used for the physical description of a given system, but the FEM model is dimensionally significantly larger than the state-space model suitable for control purposes. It is therefore necessary to reduce the FEM model.

This paper deals with the development of the FEM model of piezoelectric beam element, where the piezoelectric layers are located on the outer surface of the beam core, which is made of functionally graded material. Subsequently, the FEM model of system is transformed and reduced to state-space model by modal truncation method, which is one of the MOR methods [6]. Created state-space model is used to built feedback gain matrix and closed loop reduced state-space model is analyzed. Developed FEM model, MOR technique, state-space model and LQR control are implemented in FEM code MultiFEM.

2 PIEZOELECTRIC BEAM ELEMENT

Fig. 1 shows a two-nodal beam finite element, the core of beam is made of FGM material, piezoelectric layers with electrodes are placed on the outer surfaces of beam core. The length of the beam finite element is L^e, the width is b^e, the height FGM of the

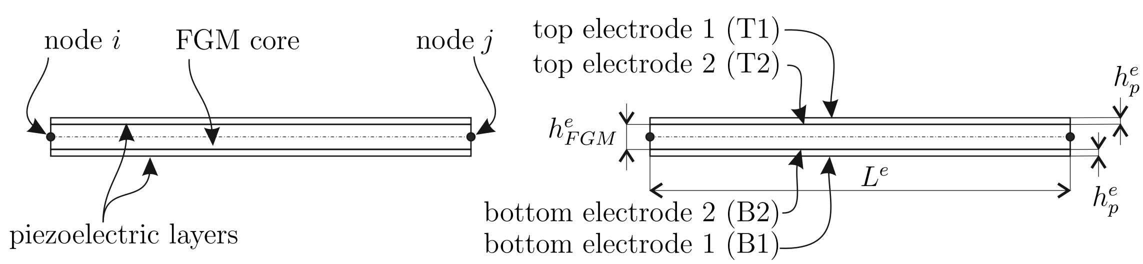

Figure 1: Beam element with FGM core and piezoelectric layers with electrodes

core is h^e_{FGM} and the height of one piezoelectric layer is h^e_p. This finite element has 10 degrees of freedom – 6 mechanical and 4 electrical, which are shown in Fig. 2. Vector of

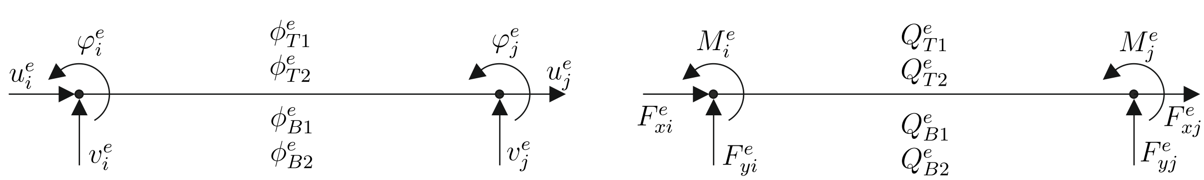

Figure 2: Piezoelectric beam element, degrees of freedom – left, element loads – right

element unknowns is defined as

$$\begin{bmatrix} \mathbf{v}^e \\ \boldsymbol{\phi}^e \end{bmatrix} = \begin{bmatrix} u^e_i & v^e_i & \varphi^e_i & u^e_j & v^e_j & \varphi^e_j & \phi^e_{T1} & \phi^e_{T2} & \phi^e_{B1} & \phi^e_{B2} \end{bmatrix}^T \tag{1}$$

and vector of element loads is defined as

$$\begin{bmatrix} \mathbf{F}^e \\ \mathbf{Q}^e \end{bmatrix} = \begin{bmatrix} F^e_{xi} & F^e_{yi} & M^e_i & F^e_{xj} & F^e_{yj} & M^e_j & Q^e_{T1} & Q^e_{T2} & Q^e_{B1} & Q^e_{B2} \end{bmatrix}^T \tag{2}$$

FEM equations of beam element with piezoelectric layers and FGM core for transient analysis have classical form

$$\begin{bmatrix} \mathbf{M}^e_{vv} & \mathbf{0} \\ \mathbf{0} & \mathbf{0} \end{bmatrix} \begin{bmatrix} \ddot{\mathbf{v}}^e \\ \ddot{\boldsymbol{\phi}}^e \end{bmatrix} + \begin{bmatrix} \mathbf{C}^e_{vv} & \mathbf{0} \\ \mathbf{0} & \mathbf{0} \end{bmatrix} \begin{bmatrix} \dot{\mathbf{v}}^e \\ \dot{\boldsymbol{\phi}}^e \end{bmatrix} + \begin{bmatrix} \mathbf{K}^e_{vv} & \mathbf{K}^e_{v\phi} \\ \mathbf{K}^e_{\phi v} & \mathbf{K}^e_{\phi\phi} \end{bmatrix} \begin{bmatrix} \mathbf{v}^e \\ \boldsymbol{\phi}^e \end{bmatrix} = \begin{bmatrix} \mathbf{F}^e \\ \mathbf{Q}^e \end{bmatrix} \tag{3}$$

The structural submatrix $\mathbf{K}^e_{vv}$ of the beam element with piezoelectric layers can be expressed in a form

$$\mathbf{K}^e_{vv} = \begin{bmatrix} k'_u & 0 & 0 & -k'_u & 0 & 0 \\ & k'_{v2} & k'_{v3} & 0 & -k'_{v2} & k_{v2} \\ \mathrm{S} & & k'_{v33} & 0 & -k'_{v3} & k_{v3} \\ & \mathrm{Y} & & k'_u & 0 & 0 \\ & & \mathrm{M} & & k'_{v2} & -k_{v2} \\ & & & & & k_{v23} \end{bmatrix} \tag{4}$$

where individual components contain the influence of FGM core stiffness and also the influence of piezoelectric layers stiffness. The calculation of components is identical for classical multilayer or FGM beam without piezoelectric layer and is described in [7]. Mass matrix $\mathbf{M}^e_{vv}$ can be calculated numerically using classical shape functions and homogenized density of FGM beam with piezoelectric layers. Damping matrix $\mathbf{C}^e_{vv}$ can be expressed as classical Rayleigh damping, i.e. as combination of stiffness and mass matrix.
The electrical submatrix $\mathbf{K}^e_{\phi\phi}$ of the beam element with piezoelectric layers can be expressed in a form

$$\mathbf{K}^e_{\phi\phi} = \begin{bmatrix} -\frac{A_p L^e \epsilon^\varepsilon}{h_p^2} & \frac{A_p L^e \epsilon^\varepsilon}{h_p^2} & 0 & 0 \\ \frac{A_p L^e \epsilon^\varepsilon}{h_p^2} & -\frac{A_p L^e \epsilon^\varepsilon}{h_p^2} & 0 & 0 \\ 0 & 0 & -\frac{A_p L^e \epsilon^\varepsilon}{h_p^2} & \frac{A_p L^e \epsilon^\varepsilon}{h_p^2} \\ 0 & 0 & \frac{A_p L^e \epsilon^\varepsilon}{h_p^2} & -\frac{A_p L^e \epsilon^\varepsilon}{h_p^2} \end{bmatrix} \tag{5}$$

where A_p is cross-sectional area of piezoelectric layer and ϵ^ε is relative permittivity at constant strain.
Piezoelectric coupling submatrices $\mathbf{K}^e_{v\phi}$ and $\mathbf{K}^e_{\phi v}$ can be expressed in form

$$\mathbf{K}^e_{v\phi} = \begin{bmatrix} -\frac{A_p d_{21} E_p}{h_p} & \frac{A_p d_{21} E_p}{h_p} & -\frac{A_p d_{21} E_p}{h_p} & \frac{A_p d_{21} E_p}{h_p} \\ 0 & 0 & 0 & 0 \\ \frac{A_y d_{21} E_p}{h_p} & -\frac{A_y d_{21} E_p}{h_p} & \frac{A_y d_{21} E_p}{h_p} & -\frac{A_y d_{21} E_p}{h_p} \\ \frac{A_p d_{21} E_p}{h_p} & -\frac{A_p d_{21} E_p}{h_p} & \frac{A_p d_{21} E_p}{h_p} & -\frac{A_p d_{21} E_p}{h_p} \\ 0 & 0 & 0 & 0 \\ -\frac{A_y d_{21} E_p}{h_p} & \frac{A_y d_{21} E_p}{h_p} & -\frac{A_y d_{21} E_p}{h_p} & \frac{A_y d_{21} E_p}{h_p} \end{bmatrix} \tag{6}$$

and

$$\mathbf{K}_{\phi v}^{e} = \begin{bmatrix} -\frac{A_p e_{21}}{h_p} & 0 & \frac{A_y e_{21}}{h_p} & \frac{A_p e_{21}}{h_p} & 0 & -\frac{A_y e_{21}}{h_p} \\ \frac{A_p e_{21}}{h_p} & 0 & -\frac{A_y e_{21}}{h_p} & -\frac{A_p e_{21}}{h_p} & 0 & \frac{A_y e_{21}}{h_p} \\ -\frac{A_p e_{21}}{h_p} & 0 & \frac{A_y e_{21}}{h_p} & \frac{A_p e_{21}}{h_p} & 0 & -\frac{A_y e_{21}}{h_p} \\ \frac{A_p e_{21}}{h_p} & 0 & -\frac{A_y e_{21}}{h_p} & -\frac{A_p e_{21}}{h_p} & 0 & \frac{A_y e_{21}}{h_p} \end{bmatrix} \tag{7}$$

where parameter A_y represents first moment of cross-section of piezoelectric layer

$$A_y = \frac{1}{2} A_p (h + h_p) \tag{8}$$

E_p is Young's modulus of piezoelectric layer, d_{21} and e_{21} are piezoelectric material properties of piezoelectric layer.

3 FEM MODEL OF PIEZOELECTRIC SYSTEM

Using equations (3) of piezoelectric beam element the final FEM equations of the piezoelectric system can be expressed in the form

$$\begin{bmatrix} \mathbf{M}_{vv} & \mathbf{0} \\ \mathbf{0} & \mathbf{0} \end{bmatrix} \begin{bmatrix} \ddot{\mathbf{v}} \\ \ddot{\boldsymbol{\phi}} \end{bmatrix} + \begin{bmatrix} \mathbf{C}_{vv} & \mathbf{0} \\ \mathbf{0} & \mathbf{0} \end{bmatrix} \begin{bmatrix} \dot{\mathbf{v}} \\ \dot{\boldsymbol{\phi}} \end{bmatrix} + \begin{bmatrix} \mathbf{K}_{vv} & \mathbf{K}_{v\phi} \\ \mathbf{K}_{\phi v} & \mathbf{K}_{\phi\phi} \end{bmatrix} \begin{bmatrix} \mathbf{v} \\ \boldsymbol{\phi} \end{bmatrix} = \begin{bmatrix} \mathbf{F} \\ \mathbf{Q} \end{bmatrix} \tag{9}$$

The matrix equation (9) can be rewritten in the form

$$\mathbf{M}_{vv}\ddot{\mathbf{v}} + \mathbf{C}_{vv}\dot{\mathbf{v}} + \mathbf{K}_{vv}\mathbf{v} + \mathbf{K}_{v\phi}\left(\boldsymbol{\phi}\right)_{\text{sens}} = \mathbf{F} - \mathbf{K}_{v\phi}\left(\boldsymbol{\phi}\right)_{\text{actu}} \tag{10}$$

$$\mathbf{K}_{\phi v}\mathbf{v} + \mathbf{K}_{\phi\phi}\left(\boldsymbol{\phi}\right)_{\text{sens}} = \left(\mathbf{Q}\right)_{\text{sens}} \tag{11}$$

$$\mathbf{K}_{\phi v}\mathbf{v} + \mathbf{K}_{\phi\phi}\left(\boldsymbol{\phi}\right)_{\text{actu}} = \left(\mathbf{Q}\right)_{\text{actu}} \tag{12}$$

where $(\boldsymbol{\phi})_{\text{sens}}$ and $(\mathbf{Q})_{\text{sens}}$ is electric potential and electric charge of sensors, respectively, and $(\boldsymbol{\phi})_{\text{actu}}$ and $(\mathbf{Q})_{\text{actu}}$ is electric potential and electric charge of actuators, respectively. If electrodes on piezoelectric sensors are short circuit, i.e. $(\boldsymbol{\phi})_{\text{sens}} = \mathbf{0}$, and electrodes on piezoelectric actuators are open circuit, i.e. $(\mathbf{Q})_{\text{actu}} = \mathbf{0}$ then equations of piezoelectric system have form

$$\mathbf{M}_{vv}\ddot{\mathbf{v}} + \mathbf{C}_{vv}\dot{\mathbf{v}} + \mathbf{K}_{vv}\mathbf{v} = \mathbf{F} - \mathbf{K}_{v\phi}\left(\boldsymbol{\phi}\right)_{\text{actu}} \tag{13}$$

$$\mathbf{K}_{\phi v}\mathbf{v} = \left(\mathbf{Q}\right)_{\text{sens}} \tag{14}$$

Equation (13) is used to calculate the deformation of the whole structure, which is loaded by external forces on the structure as well as the electric potential on the piezoelectric actuator. Equation (14) is used to calculate the electric charge, which is collected on the piezoelectric sensor.

If electrodes on piezoelectric sensors and actuators are open circuit, i.e. $(\mathbf{Q})_{\text{sens}} = \mathbf{0}$ and $(\mathbf{Q})_{\text{actu}} = \mathbf{0}$, then these equations have form

$$\mathbf{M}_{vv}\ddot{\mathbf{v}} + \mathbf{C}_{vv}\dot{\mathbf{v}} + \mathbf{K}_{vv}\mathbf{v} + \mathbf{K}_{v\phi}\left(\boldsymbol{\phi}\right)_{\text{sens}} = \mathbf{F} - \mathbf{K}_{v\phi}\left(\boldsymbol{\phi}\right)_{\text{actu}} \tag{15}$$

$$\mathbf{K}_{\phi v}\mathbf{v} + \mathbf{K}_{\phi\phi}\left(\boldsymbol{\phi}\right)_{\text{sens}} = \mathbf{0} \tag{16}$$

Equations (15) and (16) can be rewritten to form

$$\mathbf{M}_{vv}\ddot{\mathbf{v}} + \mathbf{C}_{vv}\dot{\mathbf{v}} + \left(\mathbf{K}_{vv} - \mathbf{K}_{v\phi}\mathbf{K}_{\phi\phi}^{-1}\mathbf{K}_{\phi v}\right)\mathbf{v} = \mathbf{F} - \mathbf{K}_{v\phi}\left(\boldsymbol{\phi}\right)_{\text{actu}} \tag{17}$$

$$\mathbf{K}_{\phi v}\mathbf{v} + \mathbf{K}_{\phi\phi}\left(\boldsymbol{\phi}\right)_{\text{sens}} = \mathbf{0} \tag{18}$$

Equation (17) is used to calculate the deformation of the whole structure, which is loaded by external forces on the structure as well as the electric potential on the piezoelectric actuator. Equation (18) is used to calculate the electric potential that is induced on the piezoelectric sensor.

4 MOR MODEL

The displacement of the nodal points can be expressed

$$\mathbf{v} = \mathbf{Z}.\mathbf{w} \tag{19}$$

where the matrix $\mathbf{Z}$ contains eigenshapes and $\mathbf{w}$ is vector of amplitudes of these eigenshapes. Using the transformation equation (19), equations (13) and (14) of piezoelectric system, where electrodes on piezoelectric sensors are short circuit and electrodes on piezoelectric actuators are open circuit, can be rewritten in form

$$\mathbf{M}_{vv}\mathbf{Z}\ddot{\mathbf{w}} + \mathbf{C}_{vv}\mathbf{Z}\dot{\mathbf{w}} + \mathbf{K}_{vv}\mathbf{Z}\mathbf{w} = \mathbf{F} - \mathbf{K}_{v\phi}\left(\boldsymbol{\phi}\right)_{\text{actu}} \tag{20}$$

$$\left(\mathbf{Q}\right)_{\text{sens}} = \mathbf{K}_{\phi v}\mathbf{Z}\mathbf{w} \tag{21}$$

Using orthogonality properties of mode shapes

$$\mathbf{Z}^{\mathrm{T}}\mathbf{M}_{vv}\mathbf{Z} = \mathrm{diag}(\mu_k) \tag{22}$$

$$\mathbf{Z}^{\mathrm{T}}\mathbf{K}_{vv}\mathbf{Z} = \mathrm{diag}(\mu_k\omega_k^2) \tag{23}$$

$$\mathbf{Z}^{\mathrm{T}}\mathbf{C}_{vv}\mathbf{Z} = \mathrm{diag}(2\xi_k\mu_k\omega_k) \tag{24}$$

equations (20) and (21) can be rewritten in form

$$\boldsymbol{\mu}\ddot{\mathbf{w}} + 2\boldsymbol{\xi}\boldsymbol{\mu}\boldsymbol{\omega}\dot{\mathbf{w}} + \boldsymbol{\mu}\boldsymbol{\omega}^2\mathbf{w} = \mathbf{Z}^{\mathrm{T}}\mathbf{F} - \mathbf{Z}^{\mathrm{T}}\mathbf{K}_{v\phi}\left(\boldsymbol{\phi}\right)_{\text{actu}} \tag{25}$$

$$\left(\mathbf{Q}\right)_{\text{sens}} = \mathbf{K}_{\phi v}\mathbf{Z}\mathbf{w} \tag{26}$$

where $\boldsymbol{\mu}$, $\boldsymbol{\omega}$ and $\boldsymbol{\xi}$ represent matrix of modal masses, matrix of modal frequencies and matrix of modal damping ratios of structure, respectively. Equations (25) and (26) can be rewritten into form

$$\begin{bmatrix} \dot{\mathbf{w}} \\ \ddot{\mathbf{w}} \\ (\mathbf{Q})_{\text{sens}} \end{bmatrix} = \begin{bmatrix} \mathbf{0} & \boldsymbol{I} \\ -\boldsymbol{\omega}^2 & -2\boldsymbol{\xi}\boldsymbol{\omega} \\ \mathbf{K}_{\phi v}\mathbf{Z} & \mathbf{0} \end{bmatrix} \begin{bmatrix} \mathbf{w} \\ \dot{\mathbf{w}} \end{bmatrix} + \begin{bmatrix} \mathbf{0} & \mathbf{0} \\ -\boldsymbol{\mu}^{-1}\mathbf{Z}^{\mathrm{T}}\mathbf{K}_{v\phi} & \boldsymbol{\mu}^{-1}\mathbf{Z}^{\mathrm{T}} \\ \mathbf{0} & \mathbf{0} \end{bmatrix} \begin{bmatrix} (\boldsymbol{\phi})_{\text{actu}} \\ \mathbf{F} \end{bmatrix} \tag{27}$$

Equation (27) can be formally written as state-space model

$$\dot{\mathbf{x}} = \mathbf{A}\mathbf{x} + \mathbf{B}\mathbf{u} \tag{28}$$

$$\mathbf{y} = \mathbf{C}\mathbf{x} + \mathbf{D}\mathbf{u} \tag{29}$$

where individual matrices **A**, **B**, **C** and **D** have form

$$\mathbf{A} = \begin{bmatrix} \mathbf{0} & \boldsymbol{I} \\ -\boldsymbol{\omega}^2 & -2\boldsymbol{\xi}\boldsymbol{\omega} \end{bmatrix} \qquad \mathbf{B} = \begin{bmatrix} \mathbf{0} & \mathbf{0} \\ -\boldsymbol{\mu}^{-1}\mathbf{Z}^{\mathrm{T}}\mathbf{K}_{v\phi} & \boldsymbol{\mu}^{-1}\mathbf{Z}^{\mathrm{T}} \end{bmatrix} \tag{30}$$

$$\mathbf{C} = \begin{bmatrix} \mathbf{K}_{\phi v}\mathbf{Z} & \mathbf{0} \end{bmatrix} \qquad \mathbf{D} = \begin{bmatrix} \mathbf{0} & \mathbf{0} \end{bmatrix} \tag{31}$$

and vector $\mathbf{x} = \begin{bmatrix} \mathbf{w} & \dot{\mathbf{w}} \end{bmatrix}^{\mathrm{T}}$ is state vector, $\mathbf{y} = (\mathbf{Q})_{\mathrm{sens}}$ is output vector and $\mathbf{u} = \begin{bmatrix} (\boldsymbol{\phi})_{\mathrm{actu}} & \mathbf{F} \end{bmatrix}^{\mathrm{T}}$ is input vector. If electrodes on piezoelectric sensors and actuators are open circuit, matrices **A** and **C** have shape

$$\mathbf{A} = \begin{bmatrix} \mathbf{0} & \boldsymbol{I} \\ -\boldsymbol{\omega}^2 + \mathbf{Z}^{\mathrm{T}}\mathbf{K}_{v\phi}\mathbf{K}_{\phi\phi}^{-1}\mathbf{K}_{\phi v}\mathbf{Z} & -2\boldsymbol{\xi}\boldsymbol{\omega} \end{bmatrix} \qquad \mathbf{C} = \begin{bmatrix} -\mathbf{K}_{\phi\phi}^{-1}\mathbf{K}_{\phi v}\mathbf{Z} & \mathbf{0} \end{bmatrix} \tag{32}$$

and output vector is $\mathbf{y} = (\boldsymbol{\phi})_{\mathrm{sens}}$.
When in the transformation process from the FEM model to the state-space model only selected eigenmodes and appropriate eigenfrequencies of system are considered, we obtain reduced modal truncation model.

5 LQR CONTROL

Input vector $\mathbf{u}$ can be split into external input $\mathbf{u}_{\mathrm{e}}$ and controller input $\mathbf{u}_{\mathrm{c}}$. The control for a linear system with full-state feedback, which is shown in Fig. 3, is given by proportional control

$$\mathbf{u}_{\mathrm{c}} = -\mathbf{K}\mathbf{x} \tag{33}$$

The goal of the linear quadratic control law is to design the gain matrix **K** so that the

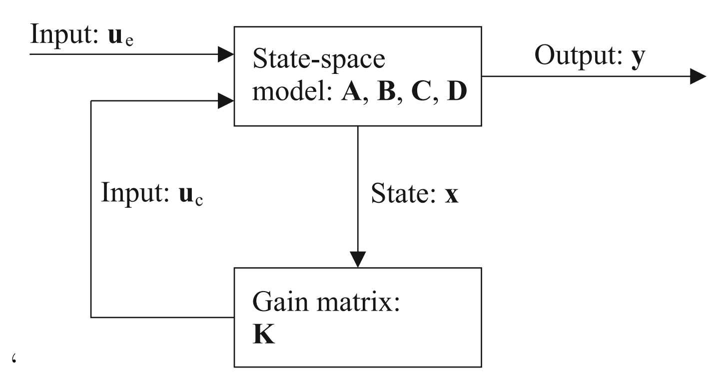

Figure 3: Control of system with full-state feedback

state of the system **x** converges to the zero state as quickly as possible, but with the least possible effort. Mathematically, this can be expressed using the so-called cost function in the form

$$J = \frac{1}{2}\int_0^\infty \left(\mathbf{x}^T\mathbf{Q}\mathbf{x} + \mathbf{u}_c^T\mathbf{R}\mathbf{u}_c\right) dt \tag{34}$$

and the goal is to construct $\mathbf{u}_c = -\mathbf{K}\mathbf{x}$ in such a way to minimize $J = \lim_{t\to\infty} J(t)$. The resulting full-state feedback controller is called a linear quadratic regulator (LQR), since it is a linear control law that minimizes a quadratic cost function to regulate the system. Matrix $\mathbf{Q}$ is positive semidefinite matrix and $\mathbf{R}$ is positive matrix and they represent weights of state and input vectors in the process of minimization of a cost function J. These matrices are often diagonal, and the diagonal elements may be tuned to change the relative importance of the control objectives.

6 NUMERICAL EXPERIMENT

The analyzed system is shown in Fig. 4. It consists of 3 beams: beam 1 and beam 2 are made of functionally graded material with variation of material properties along the length and height of the beam, beam 3 has constant material properties. A piezoelectric actuator is located on the beam 1 and a piezoelectric sensor is placed on the beam 2. The goal is to

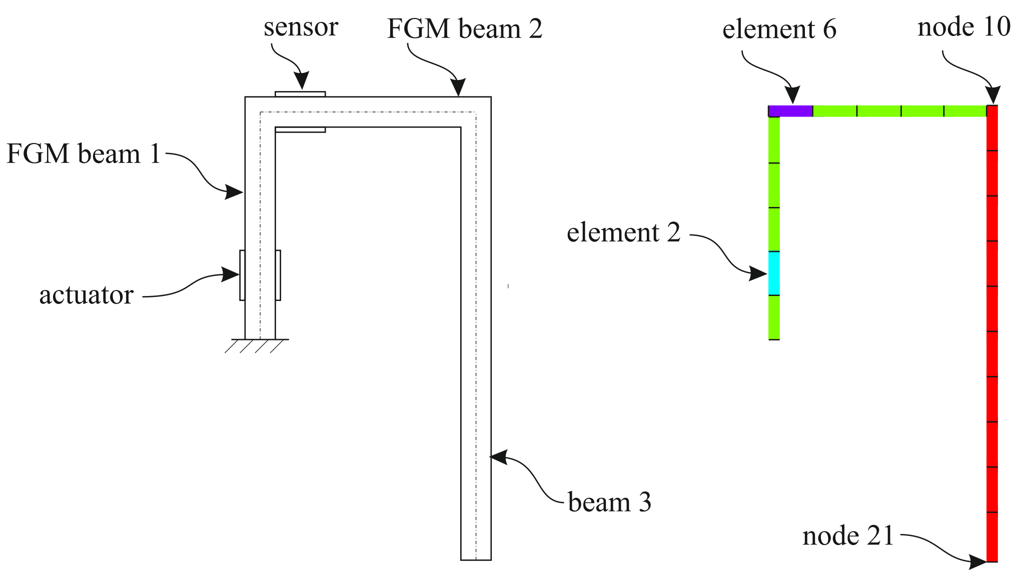

Figure 4: Piezoelectric structure with actuator and sensor – left, discretized FEM model – right

perform a FEM transient analysis of the system under defined initial conditions, to create an MOR model using the modal properties of the system, to compare the results from FEM and MOR models, to design of the linear quadratic regulator (LQR) and compare the response of the system without control and with control. Geometry parameters of beams are:

- cross-section – all beams have height and depth of cross-section 0.01 m, height of piezoelectric layers is 0.001 m and its depth is 0.01 m

- length – beam 1 and 2 have length 0.05 m and beam 3 has length 0.1 m, length of piezoelectric layers is 0.01 m

Material parameters of beams are:

- core of beam – beam 1 and 2 are made from FGM – see next subsection, beam 3 has constant material properties: $E = 319.4$ GPa, $\rho = 13989.6$ kg/m^3
- piezoelectric layer – PZT5A – see next subsection

Damping of structure is considered as Rayleigh damping with mass and stiffness constants 1×10^{-5} s^{-1} and 1×10^{-5} s, respectively.

6.1 Material properties

Beam 1 and beam 2 are made from functionally graded materials. Material of matrix (index m) is NiFe with constant density and Young's modulus and material of fibre (fibre – index f) is tungsten with constant density and Young's modulus:

- Young's modulus: $E_m = 255$ GPa, $E_f = 400$ GPa
- density: $\rho_m = 9200$ kg/m^3, $\rho_f = 19300$ kg/m^3

Volume fractions of both constituents $v_m(x, y)$ and $v_f(x, y)$ vary along the length and height of beams (x is longitudinal axis and y is transversal axis of beam 1 and beam 2) according equations:

$$v_m(x, y) = -1.\overline{3} \times 10^8 x^3 y^2 + 1333.\overline{3} x^3 + 2. \times 10^7 x^2 y^2 - 200. x^2 - 40000. y^2 + 1. \quad [\text{-}] \quad (35)$$

$$v_f(x, y) = 1.\overline{3} \times 10^8 x^3 y^2 - 1333.\overline{3} x^3 - 2. \times 10^7 x^2 y^2 + 200. x^2 + 40000. y^2 \quad [\text{-}] \quad (36)$$

Both functions of volume fractions for beam with length 0.1 m (total length of beam 1 and beam 2) and height 0.01 m are shown in Fig. 5.

Effective material properties of FGM are defined by material properties of constituents and their variations and Young's modulus and density of considered FGM have form

$$\begin{aligned} E_{\text{FGM}}(x, y) =& 1.9\overline{3} \times 10^{19} x^3 y^2 - 1.9\overline{3} \times 10^{14} x^3 - 2.9 \times 10^{18} x^2 y^2 + \\ &+ 2.9 \times 10^{13} x^2 + 5.8 \times 10^{15} y^2 + 2.55 \times 10^{11} \quad [\text{Pa}] \end{aligned} \quad (37)$$

$$\begin{aligned} \rho_{\text{FGM}}(x, y) =& 1.34667 \times 10^{12} x^3 y^2 - 1.34667 \times 10^7 x^3 - 2.02 \times 10^{11} x^2 y^2 + \\ &+ 2.02 \times 10^6 x^2 + 4.04 \times 10^8 y^2 + 9200. \quad [\text{kg/m}^3] \end{aligned} \quad (38)$$

Homogenized material properties of investigated FGM beams can be calculated by defined cross-section parameters of beams and by effective material properties and have following forms:

$$E^N_{\text{FGM}}(x) = -3.\overline{2} \times 10^{13} x^3 + 4.8\overline{3} \times 10^{12} x^2 + 3.0\overline{3} \times 10^{11} \quad [\text{Pa}] \quad (39)$$

$$E^M_{\text{FGM}}(x) = 9.\overline{6} \times 10^{13} x^3 - 1.45 \times 10^{13} x^2 + 3.42 \times 10^{11} \quad [\text{Pa}] \quad (40)$$

$$\rho_{\text{FGM}}(x) = -2.2\overline{4} \times 10^6 x^3 + 33666.\overline{6} x^2 + 12566.\overline{6} \quad [\text{kg/m}^3] \quad (41)$$

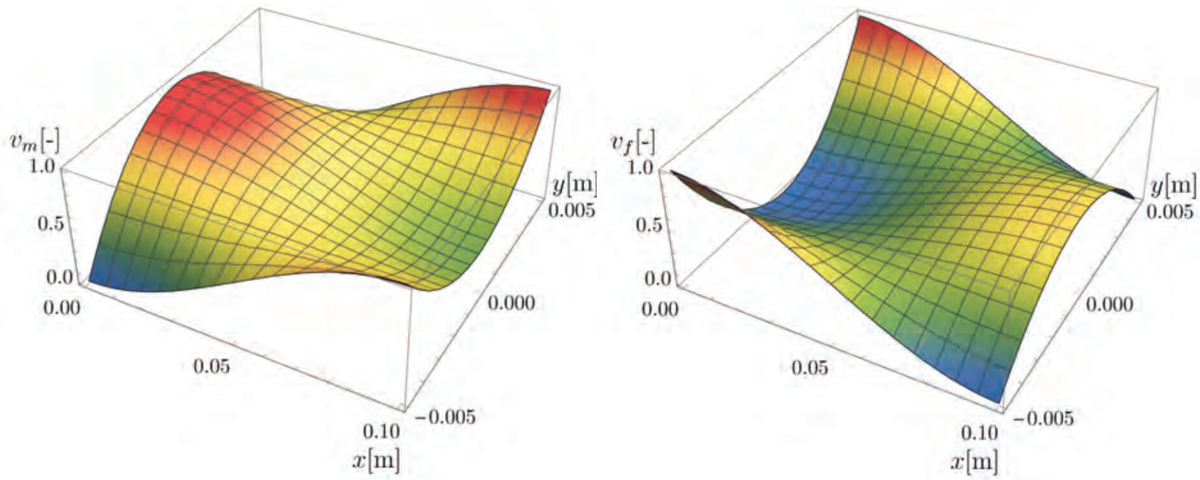

Figure 5: Volume fraction of matrix – left, volume fraction of fibre – right

$E^N_{\mathrm{FGM}}(x)$ and $E^M_{\mathrm{FGM}}(x)$ represent homogenized Young's modulus for axial loading and for bending, respectively.

Piezoelectric layers in investigated beams are made from PZT5A piezoelectric material. PZT5A is orthotropic material and has following material properties (direction of poling has index 3):

- mechanical properties:
  - Young's moduli: $E_1 = 61$ GPa, $E_2 = 61$ GPa, $E_3 = 53,2$ GPa
  - Poisson numbers: $\mu_{12} = 0.35$, $\mu_{13} = 0.38$, $\mu_{23} = 0.38$
  - shear moduli: $G_{12} = 22.6$ GPa, $G_{13} = 21.1$ GPa, $G_{23} = 21.1$ GPa
  - density: 7750 kg/m^3
- piezoelectric properties: $d_{31} = -171 \times 10^{-12}$ C/N, $d_{33} = 374 \times 10^{-12}$ C/N, $d_{15} = 584 \times 10^{-12}$ C/N, $d_{24} = 584 \times 10^{-12}$ C/N
- relative permittivity: $\epsilon^{\sigma}_{11} = 1728.8$, $\epsilon^{\sigma}_{22} = 1728.8$, $\epsilon^{\sigma}_{33} = 1694.9$

6.2 Analysis of FEM model

The initial state of the analyzed structure is defined by the static deformation of the structure, when the horizontal displacement of the free end of beam structure is prescribed - node 21, the displacement has value 5×10^{-6} m. Free vibration of structure is investigated.

The discretized FEM model is shown in Fig. 4 right. The response of the system - the vertical displacement of nodes 21 and 10 and electric charge on element 6 is shown in Fig. 6. The goal of the modal analysis is to obtain the first 4 bending eigenfrequencies and the corresponding eigenmodes of the analyzed beam structure. These eigenfrequencies and

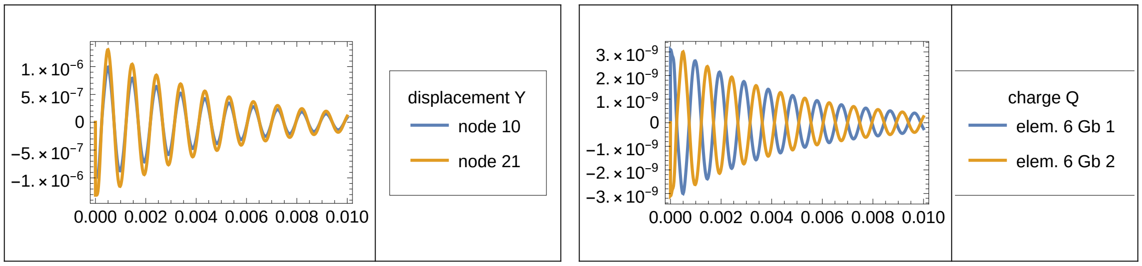

Figure 6: The response of the system, the vertical displacement of nodes 21 and 10 – left, electric charge on element 6 – right

eigenmodes are subsequently used both in the creation of a reduced model of the system and in the definition of the modal initial state of the system. The first four eigenshapes are shown in Fig. 7 and corresponding eigenfrequencies are 1040.24 Hz, 4251.05 Hz, 7256.15 Hz and 17477.4 Hz.

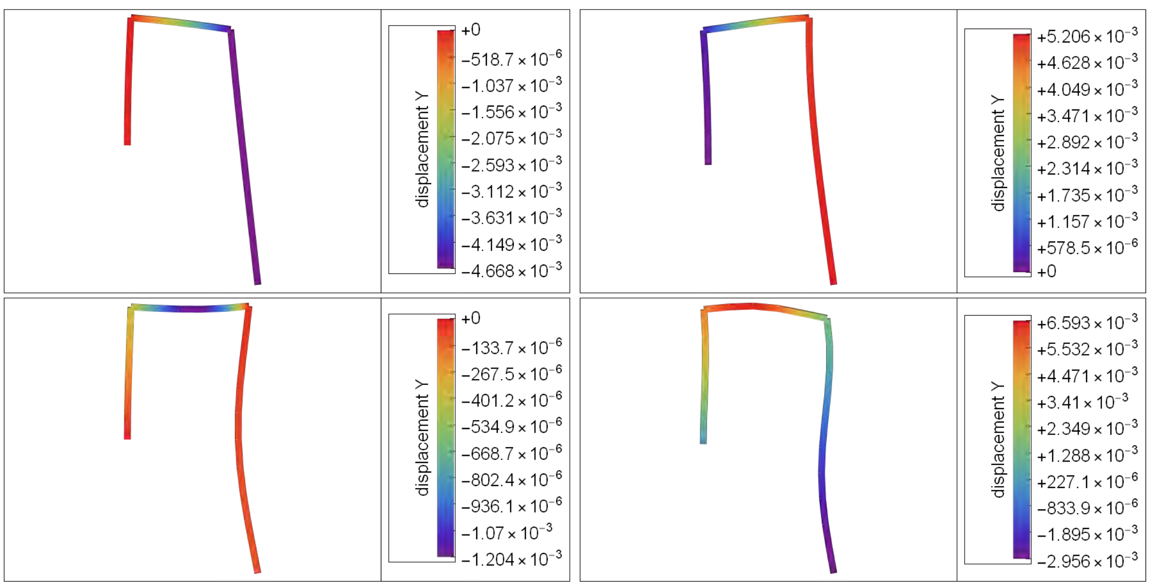

Figure 7: The first 4 bending eigenmodes

6.3 Analysis of MOR model

A reduced model was created using the modal truncation method, considering the first 4 eigenshapes of the structure shown in Fig. 7 and their corresponding natural frequencies. The created reduced state-space model was analyzed in Mathematica using the StateResponse and OutputResponse commands, which simulate state quantities and output quantities, respectively. The obtained state and output quantities from the reduced state-space model were compared with the results obtained from the FEM model – Fig. 8, where FEM results are shown by a blue line, and MOR results by a brown ring. Fig.

8 left shows the vertical displacement of the node 21 and Fig. 8 right shows the electric charge on the piezoelectric sensor – element 6. As can be seen from these results, the

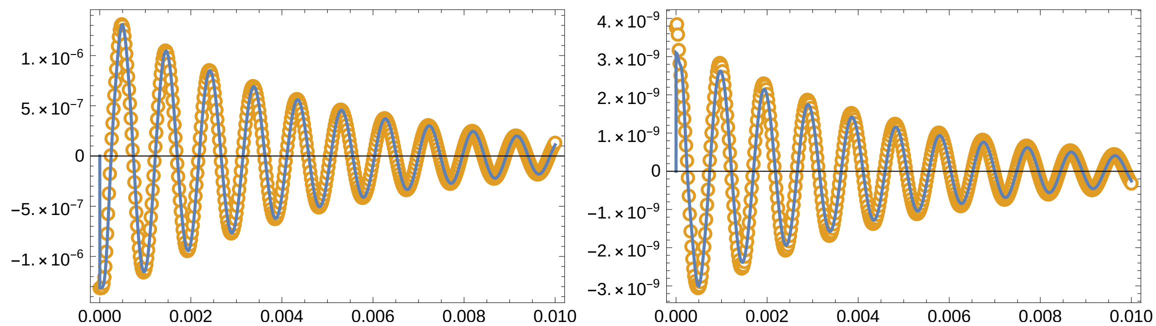

Figure 8: Results calculated by FEM model (blue line) and by MOR model (brown rings), vertical displacement of free end – left, electric charge on sensor – right

displacement as well as the electric charge obtained from the MOR simulation correspond very well with quantities obtained from the FEM analysis.

6.4 Control of MOR model

For the analyzed system an linear quadratic regulator was proposed. The output of gain matrix of regulator is the electrical voltage for the piezoelectric actuator and the input of controller is the full state of the model. The proposed LQR controller was connected with reduced state-space model and the final closed loop system was analyzed. The initial state of closed loop system was defined in the same way as in the transient FEM analysis. A comparison of a deformation of a system represented by vertical displacement of node 21 without control and a system with control is shown in Fig. 9 left, Fig. 9 right shows the electrical voltage that is applied to the piezoelectric actuator as controller output.

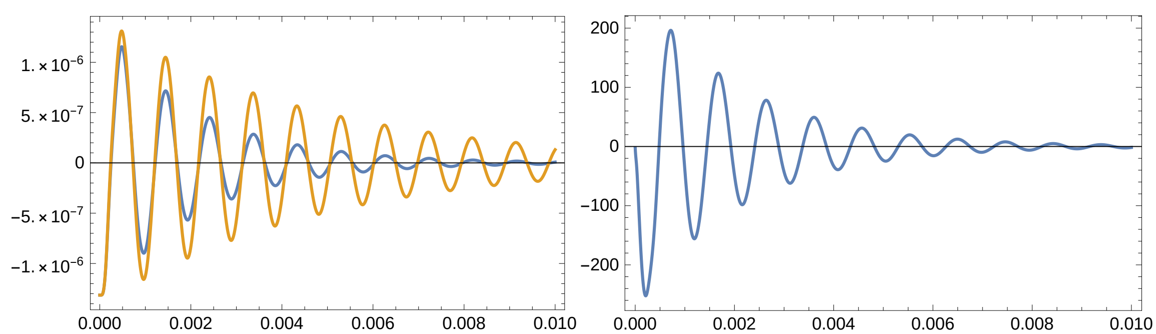

Figure 9: A comparison of a deformation of a system represented by vertical displacement of node 21 without control (brown line) and a system with control (blue line) – left, the electrical voltage applied to the piezoelectric actuator – right

7 CONCLUSIONS

The article analyzes the smart structure, which uses functionally graded materials, piezoelectric materials and modern control. In modeling such a mechatronic system, the finite element method was used as a tool to create a reference model from which it is possible to obtain modal properties of the system. Subsequently, the modal properties were used to create a reduced state-space model using the modal truncation method. Built state-space MOR model was used to design an LQR controller. All models were tested on simple numerical experiments.

ACKNOWLEDGEMENT

This work was supported by the Slovak Grant Agency: VEGA 1/0081/18, KEGA 011STU-4/2020 and APVV-19-0406.

REFERENCES

[1] Bolton, W. *Mechatronics, Electronic Control Systems in Mechanical and Electrical Engineering*. Pearson, (2015).

[2] Schwartz, M. *Encyclopedia of Smart Materials*. John Wiley & Sons, Inc., (2002).

[3] Arnau, A. *Piezoelectric Transducers and Applications*. Springer, (2008).

[4] Dorf, R. C. and Bishop, R. H. *Modern Control Systems*. Pearson, (2017).

[5] Burnett, D.S. *Finite Element Analysis: From Concepts to Applications*. Addison Wesley Publishing Company, (1987).

[6] Besselink, B. et al., A Comparison of Model Reduction Techniques from Structural Dynamics, Numerical Mathematics and Systems and Control. *Journal of Sound and Vibration* (2013) **332**:4403–4422.

[7] Kutiš, Murín, J., Belák, R. and Paulech J. Beam element with spatial variation of material properties for multiphysics analysis of functionally graded materials. *Computers & Structures* 2011 **89**:1192–1205.